

# THE INTERNAL ENERGY FOR MOLECULAR HYDROGEN IN GRAVITATIONALLY UNSTABLE PROTOPLANETARY DISKS

AARON C. BOLEY,<sup>1</sup> THOMAS W. HARTQUIST,<sup>2</sup> RICHARD H. DURISEN,<sup>1</sup> AND SCOTT MICHAEL<sup>1</sup>

*Received 2006 August 31; accepted 2007 January 4; published 2007 January 18*

## ABSTRACT

The gas equation of state may be one of the critical factors for the disk instability theory of gas giant planet formation. This Letter addresses the treatment of H<sub>2</sub> in hydrodynamic simulations of gravitationally unstable disks. In our discussion, we point out possible consequences of erroneous specific internal energy relations, approximate specific internal energy relations with discontinuities, and assumptions of constant  $\Gamma_1$ . In addition, we consider whether the ortho/para ratio for H<sub>2</sub> in protoplanetary disks should be treated dynamically as if the species are in equilibrium. Preliminary simulations indicate that the correct treatment is particularly critical for the study of gravitational instability when  $T = 30\text{--}50$  K.

*Subject headings:* accretion, accretion disks — equation of state — hydrodynamics — instabilities — molecular processes

*Online material:* color figures

## 1. INTRODUCTION

Researchers disagree on several key issues of disk evolution, particularly regarding fragmentation and planet formation, despite numerous studies of gravitational instabilities in protoplanetary disks (see Durisen et al. 2007 for a review). Recent three-dimensional radiative hydrodynamics simulations of protoplanetary disks with gravitational instabilities (GIs) demonstrate disparate evolutions, and the differences involve the importance of convection in disks, the dependence of disk cooling on metallicity, and the stability of disks to fragmentation and clump formation (Boss 2005; Cai et al. 2006; Boley et al. 2006; Mayer et al. 2006).

These disparities may be due to differences in the treatments of radiative transfer and the assumed equation of state. Our own group has undertaken systematic improvements to the Indiana University Hydrodynamics Group code in these two areas. A. C. Boley et al. (2007, in preparation) will present a new scheme for 3D radiative cooling in disks that passes a series of accuracy and reliability tests, which are suggested as a new standard for disk stability studies. Because the equation of state can severely change the outcome of a simulation (Pickett et al. 1998, 2000a), we have also implemented an internal energy that takes into account the translational, rotational, and vibrational states of H<sub>2</sub>. During its development, we noticed that in all treatments to date of planet formation by disk instability, the effects of the rotational states of H<sub>2</sub> have been, at best, only poorly approximated. The purpose of this Letter is to draw attention to possible consequences of various approximations for the internal energy of H<sub>2</sub> that are in the literature and to disseminate the correct treatment for H<sub>2</sub>. We have begun a series of simulations to investigate the severity of using the incorrect internal energies. We mention only preliminary results in this Letter, but the simulations will be fully discussed in a future paper.

This Letter is laid out as follows: In § 2 we outline the correct treatment of H<sub>2</sub> under simple conditions, i.e., no dissociation and no ionization. We discuss the ortho/para hydrogen

ratio for optically thick protoplanetary disks in § 3, and we summarize the main points of the Letter in § 4.

## 2. THERMODYNAMICS

In this section we summarize relevant thermodynamic relations. For an in-depth discussion, we refer the reader to Pathria (1996). Consider the following thermodynamic properties of an ideal gas: Let  $E$  be the internal energy for  $N$  particles,  $e$  the specific internal energy,  $\epsilon$  the internal energy density,  $p$  the pressure,  $T$  the gas temperature,  $\rho$  the gas density,  $\mu$  the mean molecular weight in proton masses,  $c_v$  the specific heat capacity at constant volume,  $Z$  the partition function for the ensemble,  $z$  the partition function for a single particle, and  $R = k/m_p$ , where  $k$  is Boltzmann's constant and  $m_p$  is the proton mass. We only consider independent contributions to the partition function from translation, rotation, and vibration represented by  $Z = Z_{\text{tran}} Z_{\text{rot}} Z_{\text{vib}} = z^N = (z_{\text{tran}} z_{\text{rot}} z_{\text{vib}})^N$ . The internal energy  $E$  and the specific internal energy  $e$  can be calculated by

$$E = NkT^2 \frac{\partial \ln z}{\partial T}, \quad e = \frac{R}{\mu} T^2 \frac{\partial \ln z}{\partial T} \quad (1)$$

for constant  $\rho$ . Because the gas is ideal,  $c_v = de/dT$ . If  $c_v$  is constant, then  $e = c_v T$ . Black & Bodenheimer (1975) calculate  $c_v$  from the Helmholtz free energy, which is valid, but then assume  $e = c_v T$ , which is invalid, because  $c_v$  is dependent on  $T$ . Other authors have followed suit (e.g., Whitehouse & Bate 2006), and this assumption could be troublesome for gas dynamics in a hydrodynamics simulation (see below). We do note that the severity of this error may depend on the state variables evolved in a given code, and only the authors who employ  $e = c_v T$  will be able to say in detail how it affects their simulations.

### 2.1. Molecular Hydrogen

Molecular hydrogen exists as para-hydrogen and as ortho-hydrogen where the proton spins are antiparallel and parallel, respectively. The partition function for para-hydrogen is

$$z_p = \sum_{j \text{ even}} (2j + 1) \exp(-j(j + 1)\theta_{\text{rot}}/T), \quad (2)$$

<sup>1</sup> Indiana University, Astronomy Department, Bloomington, IN; acboley@astro.indiana.edu.

<sup>2</sup> University of Leeds, School of Physics and Astronomy, Leeds, UK.

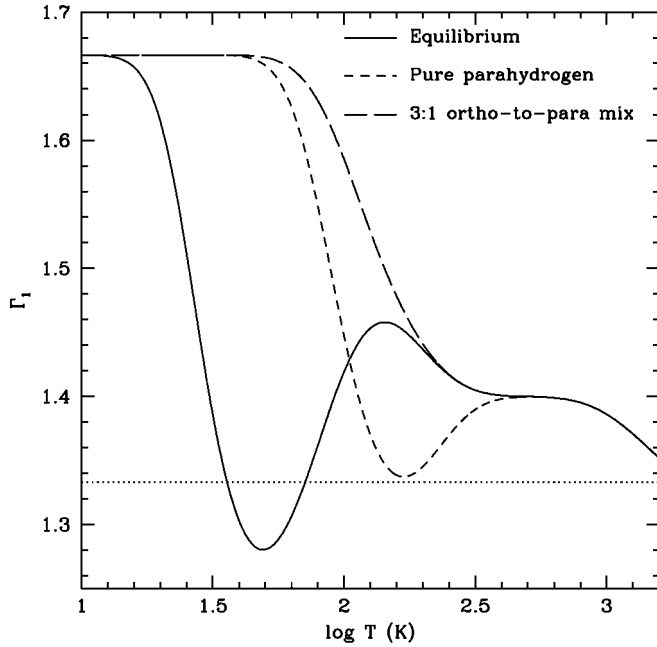


FIG. 1.—Profiles of  $\Gamma_1$  for an equilibrium mix (solid curve), para-hydrogen (short-dashed curve), and a 3 : 1 ortho/para ratio mix (long-dashed curve). The dotted line indicates  $\Gamma_1 = 4/3$ ; this figure is similar to Fig. 2 of Decampli et al. (1978). [See the electronic edition of the *Journal* for a color version of this figure.]

and the partition function for ortho-hydrogen is

$$z_o = \sum_{j \text{ odd}} 3(2j+1) \exp(-j(j+1)\theta_{\text{rot}}/T), \quad (3)$$

where  $\theta_{\text{rot}} = 85.4$  K (Black & Bodenheimer 1975). When the two species are in equilibrium,  $z_{\text{rot}} = z_p + z_o$ . However, the ortho/para ratio ( $b : a$ ) could also be frozen if no efficient mechanism for converting between the species is available. This leads to  $z_{\text{rot}} = z_p^{[a/(a+b)]} z_o^{[b/(a+b)]}$ , where  $z_o' = z_o \exp(2\theta_{\text{rot}}/T)$ . The additional exponential is required in the ortho-hydrogen partition function when the ortho and para species are at some fixed ratio to ensure that rotation only contributes to the internal energy once the rotational states are excited, i.e.,  $z_o' \rightarrow 1$  as  $T \rightarrow 0$ .

To consider the vibrational states, we approximate the molecule as an infinitely deep harmonic oscillator, where

$$z_{\text{vib}} = \frac{1}{1 - \exp(-\theta_{\text{vib}}/T)}. \quad (4)$$

Here  $\theta_{\text{vib}} = 5987$  K (Draine et al. 1983). Because we are only interested in temperatures  $T \lesssim 1500$  K where dissociation of  $\text{H}_2$  is insignificant, we can ignore differences between equation (4) and a proper  $z_{\text{vib}}$ , which would take into account the anharmonicity of the molecule and that the molecule has a finite number of vibrationally excited states.

We can use equation (1) to write the specific internal energy for  $\text{H}_2$ :

$$e(\text{H}_2) = \frac{R}{2} \left[ \frac{3}{2} T + \frac{T^2}{z_{\text{rot}}} \frac{\partial z_{\text{rot}}}{\partial T} + \theta_{\text{vib}} \frac{\exp(-\theta_{\text{vib}}/T)}{1 - \exp(-\theta_{\text{vib}}/T)} \right]. \quad (5)$$

When the gas is ideal and dissociation and ionization can

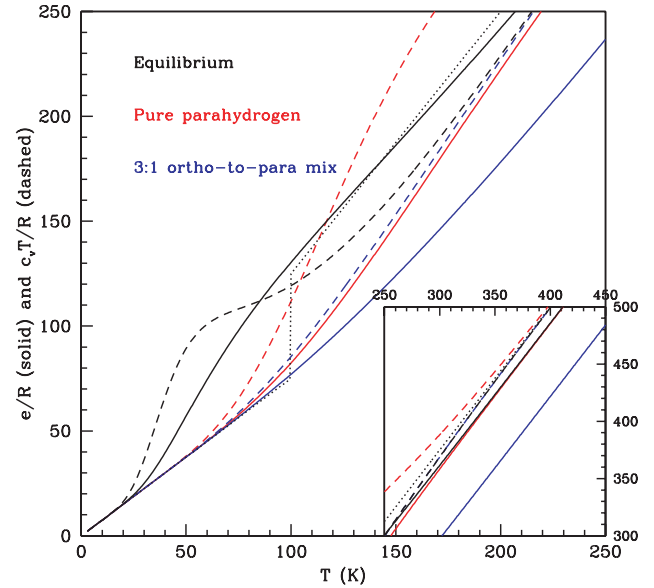


FIG. 2.—Specific internal energy profiles. The solid lines indicate the  $e$ -profiles as calculated by eq. (5), while the dashed lines indicate  $c_v T$ . The dotted line indicates a discontinuous  $e$ -profile, where  $e = 3/4RT$  for  $T < 100$  K and  $e = 5/4RT$  for  $T \geq 100$  K, as used by Boss (1984). The inset shows the behavior of the profiles at higher temperatures with the same units for the ordinate and abscissa.

be ignored, the first adiabatic exponent  $\Gamma_1 = 1 + R/\mu c_v = c_p/c_v = \gamma$  (Cox & Giuli 1968). Figure 1 indicates the  $\Gamma_1$  profiles for the equilibrium case, pure para-hydrogen, and a 3 : 1 mix, which is consistent with Figure 2 of Decampli et al. (1978), as it should be because our derivation of  $c_v$  is equivalent to theirs. The specific internal energy profiles as calculated by equation (5) are shown in Figure 2 by solid lines. Curves for  $c_v T$  are also shown in Figure 2 by dashed lines. The approximation  $e = c_v T$  gives quite different behavior from the correct  $e$ , e.g., the incorrect 3 : 1 curve most closely follows the correct pure para-hydrogen curve. The offset of the correct 3 : 1 mix profile is due to the energy stored in the parallel spins of the protons. The dotted line represents the curve  $e = 3/4RT$  for  $T < 100$  K and  $e = 5/4RT$  for  $T \geq 100$  K, which is the energy equation used by Boss (1984, 2001, 2002, 2005). Although this may be a reasonable approximation for  $e$  when the hydrogen species are in equilibrium, this approximation could be troublesome for the hydrodynamics. This is because the discontinuity guarantees that  $c_v$  becomes very large near 100 K, which forces  $\Gamma_1$  to unity. Such discontinuities may artificially favor gas giant formation by disk instability, because isothermal ( $\Gamma_1$ ) gas behavior favors fragmentation (Boss 1997, 2000; Pickett et al. 1998). Indeed, the clumping that is reported by Boss (2001) occurs at  $T \approx 100$  K (see Boss's Fig. 2). Finally, a constant  $\Gamma_1$  approximation (Pickett et al. 2003; Lodato & Rice 2004; Mayer et al. 2004, 2006; Rice et al. 2003, 2005; Mejía et al. 2005; Cai et al. 2006; Boley et al. 2006) poorly represents  $e$  in the temperature regime where Jupiter probably formed; neither  $\Gamma_1 = 5/3$  or  $7/5$  can be assumed confidently.

The dynamical effects that could result from assuming  $e = c_v T$  are evaluated by taking the temperature derivative of the dashed curves in Figure 2. The results are displayed in Figure 3, and the curves depart drastically from the correct  $\Gamma_1$  profiles. As mentioned above,  $c_v$  can be calculated from the Helmholtz free energy as is done by Black & Bodenheimer

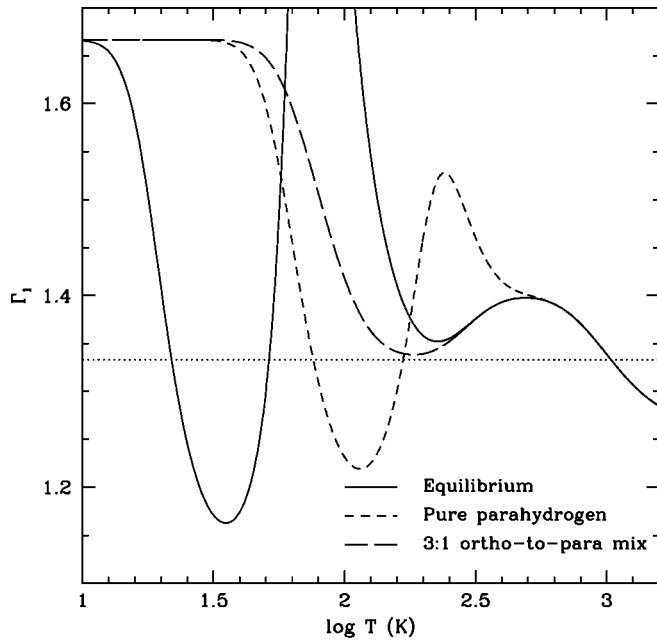


FIG. 3.—Profiles of  $\Gamma_1$  calculated by taking the temperature derivative of the dashed lines in Fig. 2. These profiles vary largely from the correct profiles in Fig. 1. The equilibrium curve's maximum is at about  $\Gamma_1 = 2.3$ . [See the electronic edition of the *Journal* for a color version of this figure.]

(1975). This makes it possible to compute  $\Gamma_1$  from  $c_v$  correctly but then evolve the gas with an erroneous effective specific heat because many hydrodynamics codes evolve  $e = \rho e$  (e.g., Black & Bodenheimer 1975; Boss 1984, 2001; Monaghan 1992; Stone & Norman 1992; Pickett 1995; Wadsley et al. 2004). If the ideal gas law  $p = R/\mu\rho T$  is assumed as well, then effective  $\Gamma_1$  profiles like those shown in Figure 3 seem to be unavoidable when  $e = c_v T$  is assumed for a temperature-dependent  $c_v$ . Because fragmentation becomes more likely as  $\Gamma_1$  becomes smaller (Rice et al. 2005; S. Michael et al. 2007, in preparation), the  $e = c_v T$  assumption should artificially make fragmentation more likely in some temperature regimes and less likely in others.

Preliminary simulations of a disk with solar composition indicate that when GIs activate between 30 and 50 K for an equilibrium ortho-para mixture, the  $e = c_v T$  simulation evolves more rapidly and has a more flocculent spiral structure than the correct  $e$  simulation for the same cooling rates. In addition, denser substructures form in some spiral arms of the  $e = c_v T$  simulation throughout the simulation, while dense substructures only form during the burst of the correct  $e$  simulation.<sup>3</sup> When the instabilities occur outside this temperature regime, the differences are diminished.

### 3. THE MOLECULAR HYDROGEN ORTHO/PARA RATIO

As indicated in § 2, the dynamical behavior of the gas is dependent on the ortho/para ratio and whether the species are in equilibrium for all  $T$ . This ratio for various astrophysical conditions has been addressed by several authors (e.g., Osterbrock 1962; Dalgarno et al. 1973; Decamp et al. 1978; Flower & Watt 1984; Sternberg & Neufeld 1999; Fuente et al. 1999; Rodríguez-Fernández et al. 2000; Flower et al. 2006), typically

in the context of interstellar clouds or photodissociation regions. However, for plausible solar nebula conditions, the ortho/para ratio has been inadequately addressed; for example, Decamp et al. (1978) used an estimate for the  $H^+$  number density that was derived originally to give the total gas-phase ion number density in gas for which dissociative recombination dominates the removal of ions. At protoplanetary disk number densities, however, ion removal should be primarily on grain surfaces if the ratio of grain surface area to hydrogen nucleon number density is the same as it is in diffuse interstellar clouds.

For protoplanetary disk conditions, the conversion between ortho- and para-hydrogen is principally due to protonated ions such as  $H_3^+$ . Consequently, we will assume that all ionizations lead to  $H_3^+$  formation. Another possible conversion mechanism is through interactions between  $H_2$  and grains; however, this conversion might only be significant when the temperature drops below about 30 K (Le Bourlot 2000).

Consider the balance between  $H_3^+$  production by cosmic rays (CRs) and  $H_3^+$  depletion by dust grains:

$$\zeta n(H_2) = n_g \pi a^2 v n_i, \quad (6)$$

where  $n(H_2)$ ,  $n_i$ , and  $n_g$  are the  $H_2$ ,  $H_3^+$ , and grain number densities, respectively,  $\zeta$  is the ionization rate by CRs and other energetic particles (EPs),  $a$  is the average radius of the grains, and  $v$  is the thermal velocity of  $H_3^+$ . If we assume standard interstellar extinction, then  $\sigma = n(H_2)/n_g \pi a^2 \approx 10^{21} \text{ cm}^{-2}$ , but as we discuss below, this number is ambiguous. The  $\zeta$  appropriate for a protoplanetary disk is also ambiguous. CRs and stellar EPs are important in ionizing the disk surface (Desch 2004; Dullemond et al. 2007), but because these particles are attenuated exponentially with a scale length of about 100 g  $\text{cm}^{-2}$  (Umebayashi & Nakano 1981), stellar EPs probably do not contribute to  $n_i$ . Moreover, protostellar winds could lead to a significant reduction of  $\zeta$  in analogy to CR modulation by the solar wind (Webber 1998). However, at a surface density of roughly 380 g  $\text{cm}^{-2}$ , EP production by  $^{26}\text{Al}$  decay is as important as CRs with  $\zeta \sim 10^{-19} \text{ s}^{-1}$  (Stepinski 1992). It is likely that  $10^{-19} \text{ s}^{-1} < \zeta < 10^{-17} \text{ s}^{-1}$ . For our estimate we adopt the interstellar rate  $\zeta = 10^{-17} \text{ s}^{-1}$  (Spitzer & Tomasko 1968). Using these numbers in equation (6) and adopting a thermal velocity of 1 km  $\text{s}^{-1}$ ,  $n_i \approx 0.1 \text{ cm}^{-3}$ . By adopting a collisional rate coefficient  $\alpha = 1 \times 10^{-9} \text{ cm}^3 \text{ s}^{-1}$  for the  $H_3^+$  interaction with  $H_2$  (Walmsley et al. 2004), the lower limit timescale for ortho- and para-hydrogen to reach equilibrium is  $t_e = (\alpha n_i)^{-1} = 300 \text{ yr}$ .

The equilibrium timescale is short enough that the ortho/para ratio can thermalize in the lifetime of a disk, but the equilibrium timescale is longer than the dynamical timescale inside about 40 AU: ortho- and para-hydrogen should be treated as independent species for hydrodynamic simulations of young protoplanetary disks.

What ortho/para ratio should a dynamicist assume for gravitationally unstable protoplanetary disk simulations? The answer is uncertain. Vertical and radial stirring induced by shock bores (Boley & Durisen 2006), which could possibly lead to mixing of the low-altitude disk interior with the high-altitude photodissociation region in the disk atmosphere (Dullemond et al. 2007), will transport gas through different temperature regimes on dynamic timescales. This could lead to nonthermalized ortho/para ratios like those that are measured from  $H_2$  rotational transition lines in some photodissociation regions (Fuente et al. 1999; Rodríguez-Fernández et al. 2000) and in Neptune's stratosphere (Fouchet et al. 2003). Moreover, ac-

<sup>3</sup> The evolution of these simulations can be viewed at <http://westworld.astro.indiana.edu>. Click on the link titled "H2 ortho-para equilibrium tests" under the "Movies" tab.

cretion of the outer disk will bring material with a cold history into warmer regions of the disk. It is unclear whether the ortho/para ratio of, say, 15 K gas will be thermalized with  $z_o/z_p \approx 0$  or whether the ortho/para ratio will be 3 : 1, which is the expected ratio for H<sub>2</sub> formation on cold grains (Flower et al. 2006). Unfortunately, the ortho/para ratio may be critical to the evolution of a protoplanetary disk. As can be seen in Figure 1, the pure para-hydrogen mix has a  $\Gamma_1$  that approaches 4/3 for  $T \approx 160$  K. This could make the 160 K regime the most likely region of the disk to fragment because, as  $\Gamma_1$  decreases, it becomes harder for the gas to support itself against local gravitational and hydrodynamic stresses (Rice et al. 2005; S. Michael et al. 2007, in preparation). Hydrodynamicists need to consider ortho/para ratios between pure para-hydrogen and 3 : 1 because of our ignorance of this ratio in protoplanetary disks.

The above discussion is based on the assumption that  $\sigma \approx 10^{21} \text{ cm}^{-2}$ , which is probably reasonable for very young protoplanetary disks but may not be reasonable for disks with ages of about 1 Myr. Grain growth and dust settling may significantly lower the value of  $\sigma$  by depleting the total grain area (e.g., Sano et al. 2000). Because models of T Tauri disks must take into account the effects of grain growth in order to match observed spectral energy distributions (D'Alessio et al. 2001, 2006; Furlan et al. 2006), there may be a period in a disk's evolution when the ortho- and para-hydrogen change from dynamically independent species to species in statistical equilibrium. Such a transition may also take place at certain radii in a disk, e.g., near edges of a dead zone (Gammie 1996). As indicated by Figure 1, a transition to statistical equilibrium could have significant dynamical consequences for disk evolution and may induce clump formation by GIs.

#### 4. SUMMARY

The effects of the rotational states of H<sub>2</sub> must be explicitly modeled in hydrodynamical simulations of protoplanetary disks. Constant  $\Gamma_1$  approximations are insufficient for modeling the dynamic behavior of the gas because they ignore the transition from a  $\Gamma_1 = 5/3$  gas to a  $\Gamma_1 = 7/5$  gas. This transition probably took place near Jupiter's location in the young solar nebula. Discontinuous  $e(T)$  assumptions or the  $e = c_v T$  approximation could lead to severe errors in the behavior of the gas, including artificially driving  $\Gamma_1 \rightarrow 1$ .

Our estimates indicate that ortho- and para-hydrogen should be treated as separate species in hydrodynamics simulations of young protoplanetary disks because the timescale to thermalize the ortho/para ratio is longer than a dynamic timescale. However, a reasonable approximation to the ortho/para ratio in young protoplanetary disks is ambiguous. Moreover, as a disk evolves, there may be a transition in the behavior of ortho- and para-hydrogen from independent species to statistical equilibrium, which might trigger disk fragmentation. Hydrodynamicists should consider a range of ortho/para ratios and the equilibrium case until this ambiguity is resolved.

We thank J. M. C. Rawlings, A. Dalgarno, and an anonymous referee for useful discussions and comments. A. C. B. was supported by a NASA Graduate Student Researchers Program fellowship. R.H.D.'s and S.M.'s contributions were supported by NASA grant NNG05GN11G. The Indiana-Leeds collaboration has been supported in part by PPARC grants funding travel to and subsistence costs in Leeds.

#### REFERENCES

- Black, D. C., & Bodenheimer, P. 1975, *ApJ*, 199, 619  
 Boley, A. C., & Durisen, R. H. 2006, *ApJ*, 641, 534  
 Boley, A. C., Mejía, A. C., Durisen, R. H., Cai, K., Pickett, M. K., & D'Alessio, P. 2006, *ApJ*, 651, 517  
 Boss, A. P. 1984, *ApJ*, 277, 768  
 ———. 1997, *Science*, 276, 1836  
 ———. 2000, *ApJ*, 536, L101  
 ———. 2001, *ApJ*, 563, 367  
 ———. 2002, *ApJ*, 576, 462  
 ———. 2005, *ApJ*, 629, 535  
 Cai, K., Durisen, R. H., Michael, S., Boley, A. C., Mejía, A. C., Pickett, M. K., & D'Alessio, P. 2006, *ApJ*, 636, L149  
 Cox, J. P., & Giuli, R. T. 1968, *Principles of Stellar Structure* (New York: Gordon & Breach)  
 D'Alessio, P., Calvet, N., & Hartmann, L. 2001, *ApJ*, 553, 321  
 D'Alessio, P., Calvet, N., Hartmann, L., Franco-Hernández, R., & Servín, H. 2006, *ApJ*, 638, 314  
 Dalgarno, A., Black, A. H., & Weisheit, J. C. 1973, *Astrophys. Lett.*, 14, 77  
 Decampli, W. M., Cameron, A. G. W., Bodenheimer, P., & Black, D. C. 1978, *ApJ*, 223, 854  
 Desch, S. J. 2004, *ApJ*, 608, 509  
 Draine, B. T., Roberge, W. G., & Dalgarno, A. 1983, *ApJ*, 264, 485  
 Dullemond, C. P., Hollenbach, D., Kamp, I., & D'Alessio, P. D. 2007, in *Protostars and Planets V*, ed. B. Reipurth, D. Jewitt, & K. Keil (Tucson: Univ. Arizona Press), 555  
 Durisen, R. H., Boss, A. P., Mayer, L., Nelson, A. F., Quinn, T., & Rice, W. K. M. 2007, in *Protostars and Planets V*, ed. B. Reipurth, D. Jewitt, & K. Keil (Tucson: Univ. Arizona Press), 607  
 Flower, D. R., Pineau des Forêts, G., & Walmsley, C. M. 2006, *A&A*, 449, 621  
 Flower, D. R., & Watt, G. D. 1984, *MNRAS*, 209, 25  
 Fouchet, T., Lellouch, E., & Feuchtgruber, H. 2003, *Icarus*, 161, 127  
 Fuente, A., Martín-Pintado, J., Rodríguez-Fernández, N. J., Rodríguez-Franco, A., de Vicente, P., & Kunze, D. 1999, *ApJ*, 518, L45  
 Furlan, E., et al. 2006, *ApJS*, 165, 568  
 Gammie, C. F. 1996, *ApJ*, 457, 355  
 Le Bourlot, J. 2000, *A&A*, 360, 656  
 Lodato, G., & Rice, W. K. M. 2004, *MNRAS*, 351, 630  
 Mayer, L., Lufkin, G., Quinn, T., & Wadsley, J. 2006, *ApJL*, submitted (astro-ph/0606361)  
 Mayer, L., Quinn, T., Wadsley, J., & Stadel, J. 2004, *ApJ*, 609, 1045  
 Mejía, A. C., Durisen, R. H., Pickett, M. K., & Cai, K. 2005, *ApJ*, 619, 1098  
 Monaghan, J. J. 1992, *ARA&A*, 30, 543  
 Osterbrock, D. E. 1962, *ApJ*, 136, 359  
 Pathria, R. K. 1996, *Statistical Mechanics* (2nd ed.; Oxford: Butterworth-Heinemann)  
 Pickett, B. K. 1995, Ph.D. thesis, Indiana Univ.  
 Pickett, B. K., Cassen, P., Durisen, R. H., & Link, R. 1998, *ApJ*, 504, 468  
 ———. 2000a, *ApJ*, 529, 1034  
 Pickett, B. K., Mejía, A. C., Durisen, R. H., Cassen, P. M., Berry, D. K., & Link, R. P. 2003, *ApJ*, 590, 1060  
 Rice, W. K. M., Armitage, P. J., Bate, M. R., & Bonnell, I. A. 2003, *MNRAS*, 339, 1025  
 Rice, W. K. M., Lodato, G., & Armitage, P. J. 2005, *MNRAS*, 364, L56  
 Rodríguez-Fernández, N. J., Martín-Pintado, J., de Vicente, P., Fuente, A., Hüttermeister, S., Wilson, T. L., & Kunze, D. 2000, *A&A*, 356, 695  
 Sano, T., Miyama, S. M., Umebayashi, T., & Nakano, T. 2000, *ApJ*, 543, 486  
 Spitzer, L. J., & Tomasko, M. G. 1968, *ApJ*, 152, 971  
 Stepinski, T. F. 1992, *Icarus*, 97, 130  
 Sternberg, A., & Neufeld, D. A. 1999, *ApJ*, 516, 371  
 Stone, J. M., & Norman, M. L. 1992, *ApJS*, 80, 753  
 Umebayashi, T., & Nakano, T. 1981, *PASJ*, 33, 617  
 Wadsley, J. W., Stadel, J., & Quinn, T. 2004, *NewA*, 9, 137  
 Walmsley, C. M., Flower, D. R., & Pineau des Forêts, G. 2004, *A&A*, 418, 1035  
 Webber, W. R. 1998, *ApJ*, 506, 329  
 Whitehouse, S. C., & Bate, M. R. 2006, *MNRAS*, 367, 32

ERRATUM: “THE INTERNAL ENERGY FOR MOLECULAR HYDROGEN IN GRAVITATIONALLY UNSTABLE PROTOPLANETARY DISKS” (ApJ, 656, L89 [2007])

AARON C. BOLEY, THOMAS W. HARTQUIST, RICHARD H. DURISEN, AND SCOTT MICHAEL

In the above-mentioned Letter, we stated that Boss uses a discontinuous internal energy for  $H_2$ , where  $H_2$  contributes  $3kT/4m_p$  to the specific internal energy  $e$  for  $T \leq 100$  K and  $5kT/4m_p$  for  $T > 100$  K, based on his own citations to A. P. Boss (ApJ, 277, 768 [1984]). It was brought to our attention by A. P. Boss (2007, private communication) that he now uses a quadratic interpolation for  $e$  between 100 and 200 K (see Fig. 1, *left panel*). This change is not mentioned in the literature but is alluded to in A. P. Boss (ApJ, 346, 336 [1989]). According to Boss, the interpolation has been used in all his simulations since Boss (1989).

In Figure 1 (*right panel*), we also illustrate the consequences for  $\Gamma_1$  of Boss’s latest  $e$  approximation by calculating the specific heat at constant volume  $c_v = de/dT$  and by relating that to  $\Gamma_1$  (see J. P. Cox & R. T. Giuli, *Principles of Stellar Structure* [New York: Gordon & Breach, 1968]). This curve is compared with curves for pure para-hydrogen (*short-dashed curve*), a 3 : 1 ortho/para-hydrogen mixture (*long-dashed curve*), where the species are treated as independent, and an equilibrium mixture (*solid curve*). Because fragmentation becomes more likely as  $\Gamma_1$  is lowered (W. K. M. Rice, G. Lodato, & P. J. Armitage, MNRAS, 364, L56 [2005]), Boss’s approximation between 100 and 200 K is likely to make his disks susceptible to fragmentation for that temperature range.

We would like to thank A. P. Boss for his discussions and clarification of his code.

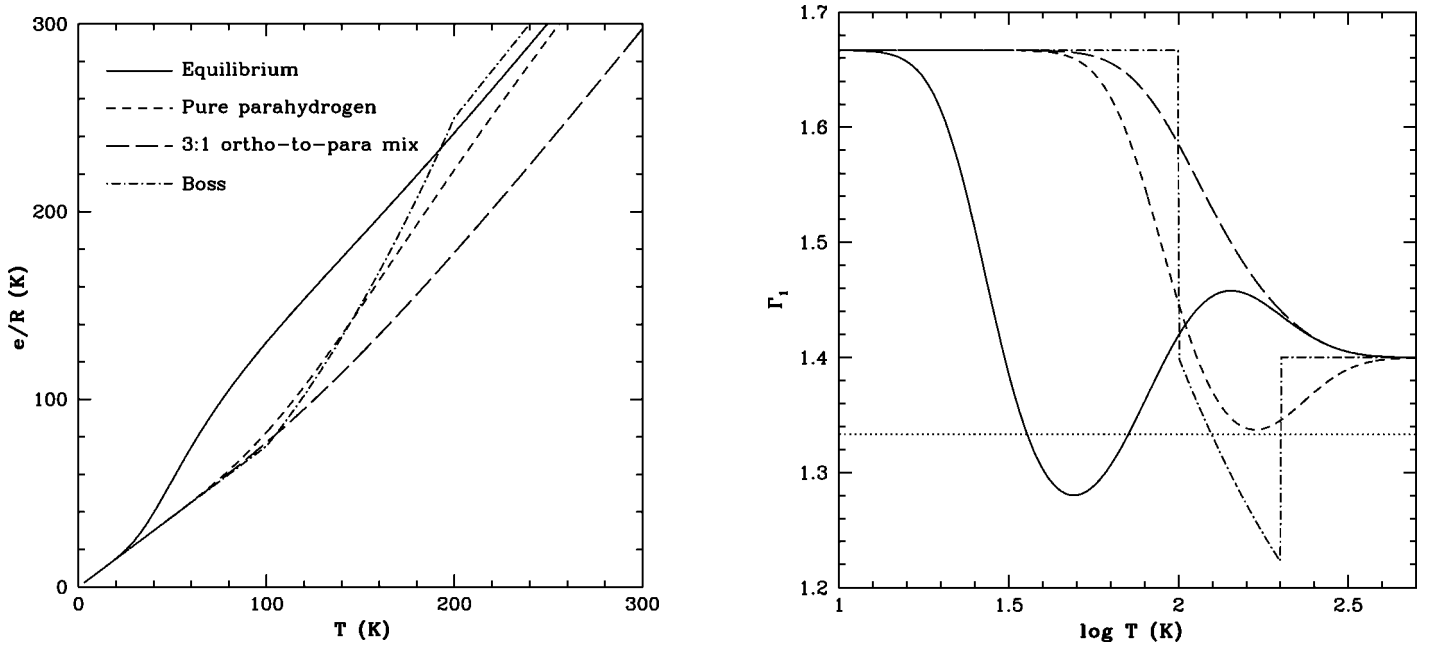


FIG. 1.—*Left*: Profiles of  $e$  for an equilibrium mix (*solid curve*), pure para-hydrogen (*short-dashed curve*), and a 3 : 1 ortho/para ratio mix (*long-dashed curve*). The dot-dashed curve indicates the approximation used by Boss. *Right*: Corresponding  $\Gamma_1$  profiles for each curve in the left panel. The dotted line indicates  $\Gamma_1 = 4/3$ .